Science
AAAS

A Circadian Rhythm Orchestrated by Histone Deacetylase 3 Controls Hepatic Lipid Metabolism

Dan Feng, *et al.*

Science **331**, 1315 (2011);
DOI: 10.1126/science.1198125

Science (print ISSN 0036-8075; online ISSN 1095-9203) is published weekly, except the last week in December, by the American Association for the Advancement of Science, 1200 New York Avenue NW, Washington, DC 20005.

Exercising control over molecular reactivity by confinement has great potential for both understanding and measuring complex chemical reactions (*40*, *41*). Regioselective photoreactions between individual molecules by molecular design and self-assembly with in situ monitoring are powerful demonstrations of chemical control via the local environment (*7*, *42*, *43*). The extraordinary resolution of the STM enables monitoring molecular motions and reactions. Controlling the chemical environment and monitoring such selective reactions between individual molecules will be important elements in directing chemistry with this approach.

References and Notes

1. R. K. Smith *et al.*, *J. Am. Chem. Soc.* **128**, 9266 (2006).
2. D. I. Gittins, D. Bethell, D. J. Schiffrin, R. J. Nichols, *Nature* **408**, 67 (2000).
3. A. Vaish *et al.*, *ACS Chem. Neurosci.* **1**, 495 (2010).
4. M. T. Cygan *et al.*, *J. Am. Chem. Soc.* **120**, 2721 (1998).
5. A. M. Moore *et al.*, *Nano Lett.* **5**, 2292 (2005).
6. P. S. Weiss, *Acc. Chem. Res.* **41**, 1772 (2008).
7. Z. J. Donhauser *et al.*, *Science* **292**, 2303 (2001).
8. A. M. Moore *et al.*, *J. Am. Chem. Soc.* **129**, 10352 (2007).
9. S. J. van der Molen *et al.*, *Nano Lett.* **9**, 76 (2009).
10. W. R. Browne *et al.*, *J. Phys. Chem. C* **112**, 1183 (2008).
11. S. W. Wu, N. Ogawa, W. Ho, *Science* **312**, 1362 (2006).
12. A. S. Kumar *et al.*, *Nano Lett.* **8**, 1644 (2008).
13. J. E. Anthony, *Chem. Rev.* **106**, 5028 (2006).
14. H. Bouas-Laurent, A. Castellan, J.-P. Desvergne, R. Lapouyade, *Chem. Soc. Rev.* **29**, 43 (2000).
15. D. K. James, J. M. Tour, *Chem. Mater.* **16**, 4423 (2004).
16. J. Reichert *et al.*, *Phys. Rev. Lett.* **88**, 176804 (2002).
17. D. Käfer, G. Witte, P. Cyganik, A. Terfort, C. Wöll, *J. Am. Chem. Soc.* **128**, 1723 (2006).
18. M. H. Zareie, J. Barber, A. M. McDonagh, *J. Phys. Chem. B* **110**, 15951 (2006).
19. M. A. Fox, M. D. Wooten, *Langmuir* **13**, 7099 (1997).
20. Z. J. Donhauser, D. W. Price II, J. M. Tour, P. S. Weiss, *J. Am. Chem. Soc.* **125**, 11462 (2003).
21. A. M. Moore *et al.*, *J. Am. Chem. Soc.* **128**, 1959 (2006).
22. E. Delamarche, B. Michel, H. A. Biebuyck, C. Gerber, *Adv. Mater.* **8**, 719 (1996).
23. T. Ishida *et al.*, *Langmuir* **13**, 3261 (1997).
24. H. D. Becker, *Chem. Rev.* **93**, 145 (1993).
25. T. Wolff, N. Müller, G. von Bünau, *J. Photochem.* **22**, 61 (1983).
26. H. D. Becker, K. Andersson, *J. Photochem.* **26**, 75 (1984).
27. D. R. Maulding, B. G. Roberts, *J. Org. Chem.* **34**, 1734 (1969).
28. M. H. Zareie, H. Ma, B. W. Reed, A. K. Y. Jen, M. Sarikaya, *Nano Lett.* **3**, 139 (2003).
29. R. F. Dou *et al.*, *Langmuir* **22**, 3049 (2006).
30. C. Gonzalez, E. C. Lim, *Chem. Phys. Lett.* **322**, 382 (2000).
31. N. J. Brewer, S. Janusz, K. Critchley, S. D. Evans, G. J. Leggett, *J. Phys. Chem. B* **109**, 11247 (2005).
32. P. A. Lewis *et al.*, *J. Am. Chem. Soc.* **126**, 12214 (2004).
33. J. U. Nielsen, M. J. Esplandiu, D. M. Kolb, *Langmuir* **17**, 3454 (2001).
34. V. Iancu, S. W. Hla, *Proc. Natl. Acad. Sci. U.S.A.* **103**, 13718 (2006).
35. Other proposed mechanisms for switching have included relative ring rotation. The calculated barrier to rotation about the ethynyl bond in MPEA is only ~1 kcal mol^{-1} (fig. S2), similar to the value calculated for phenyl ring rotation in OPEs, so the observed stability of the conductance status is inconsistent with ring rotation being responsible for conductance switching.
36. P. S. Weiss, D. M. Eigler, *Phys. Rev. Lett.* **71**, 3139 (1993).
37. I. B. Berlman, *Handbook of Fluorescence Spectra of Aromatic Molecules* (Academic Press, New York, 1971).
38. M. A. Fox, S. Olive, *Science* **205**, 582 (1979).
39. M. A. Meador, H. Hart, *J. Org. Chem.* **54**, 2336 (1989).
40. S. P. Sullivan, A. Schnieders, S. K. Mbugua, T. P. Beebe Jr., *Langmuir* **21**, 1322 (2005).
41. M. F. Perutz, A. J. Wilkinson, M. Paoli, G. G. Dodson, *Annu. Rev. Biophys. Biomol. Struct.* **27**, 1 (1998).
42. C. Chen, C. A. Bobisch, W. Ho, *Science* **325**, 981 (2009).
43. T. Ye *et al.*, *ACS Nano* **4**, 3697 (2010).

44. We thank S. Claridge for insightful discussions and the U.S. Department of Energy (no. DE-FG02-07ER15877), the NSF, the Air Force Office of Scientific Research, and the Kavli Foundation for financial support.

Supporting Online Material

www.sciencemag.org/cgi/content/full/331/6022/1312/DC1
Materials and Methods
SOM Text
Figs. S1 to S3
References

23 November 2010; accepted 2 February 2011
10.1126/science.1200830

A Circadian Rhythm Orchestrated by Histone Deacetylase 3 Controls Hepatic Lipid Metabolism

Dan Feng,[1]* Tao Liu,[2]* Zheng Sun,[1] Anne Bugge,[1] Shannon E. Mullican,[1] Theresa Alenghat,[1] X. Shirley Liu,[2] Mitchell A. Lazar[1]†

Disruption of the circadian clock exacerbates metabolic diseases, including obesity and diabetes. We show that histone deacetylase 3 (HDAC3) recruitment to the genome displays a circadian rhythm in mouse liver. Histone acetylation is inversely related to HDAC3 binding, and this rhythm is lost when HDAC3 is absent. Although amounts of HDAC3 are constant, its genomic recruitment in liver corresponds to the expression pattern of the circadian nuclear receptor Rev-erbα. Rev-erbα colocalizes with HDAC3 near genes regulating lipid metabolism, and deletion of HDAC3 or Rev-erbα in mouse liver causes hepatic steatosis. Thus, genomic recruitment of HDAC3 by Rev-erbα directs a circadian rhythm of histone acetylation and gene expression required for normal hepatic lipid homeostasis.

In mammals, metabolic processes in peripheral organs display robust circadian rhythms, coordinated with the daily cycles of light and nutrient availability (*1*, *2*). Circadian misalignment causes metabolic dysfunction, and people engaged in night-shift work suffer from higher incidences of obesity, diabetes, and metabolic syndrome (*3*–*5*). The molecular basis of this is unknown, but genetic disruption of circadian clock components in mice leads to altered glucose and lipid metabolism (*6*–*10*).

Gene expression profiles in multiple metabolic organs have revealed a circadian control of the transcriptome, which might be mediated by regulation of histone acetylation (*11*–*13*) that alters the structure of the epigenome. Regulation of histone acetylation is complex, involving multiple histone acetyltransferases (HATs) and histone deacetylases (HDACs) (*14*). Histone deacetylase 3 (HDAC3) functions in the regulation of circadian rhythm and glucose metabolism (*15*). We report diurnal recruitment of HDAC3 to the mouse liver genome detected by chromatin immunoprecipitation with an HDAC3-specific antibody (fig. S1) and massively parallel DNA sequencing (ChIP-seq).

At ZT10 [where ZT is Zeitgeber time (light on at ZT0 and off at ZT12)], in the light period when mice are inactive, HDAC3 bound to over 14,000 sites in adult mouse liver (the HDAC3 ZT10 cistrome) (fig. S2A); a majority of these binding sites were distant from transcription start sites (TSS) or present in introns (fig. S2, B and C). However, at ZT22, in the dark period when mice are active and feeding, the HDAC3 signal was dramatically reduced at ZT10 sites, with only 120 specific peaks (Fig. 1A and figs. S2, A and D, and S3). HDAC3 recruitment oscillated in a 24-hour cycle (Fig. 1B), and this rhythm was retained in constant darkness (Fig. 1C), suggesting that it was controlled by the circadian clock. The liver clock is entrained by food intake (*16*), and, indeed, the pattern of HDAC3 enrichment was reversed when food was provided only during the light period (Fig. 1D), further supporting the conclusion that the rhythm of HDAC3 genomic recruitment was controlled by the circadian clock.

Despite its known role in histone deacetylation and transcriptional repression, HDAC3

[1]Division of Endocrinology, Diabetes, and Metabolism, Department of Medicine, Department of Genetics, and the Institute for Diabetes, Obesity, and Metabolism (IDOM), University of Pennsylvania School of Medicine, Philadelphia, PA 19104, USA. [2]Department of Biostatistics and Computational Biology, Dana-Farber Cancer Institute and Harvard School of Public Health, Boston, MA 02115, USA.

*These authors contributed equally to this work.
†To whom correspondence should be addressed. E-mail: lazar@mail.med.upenn.edu

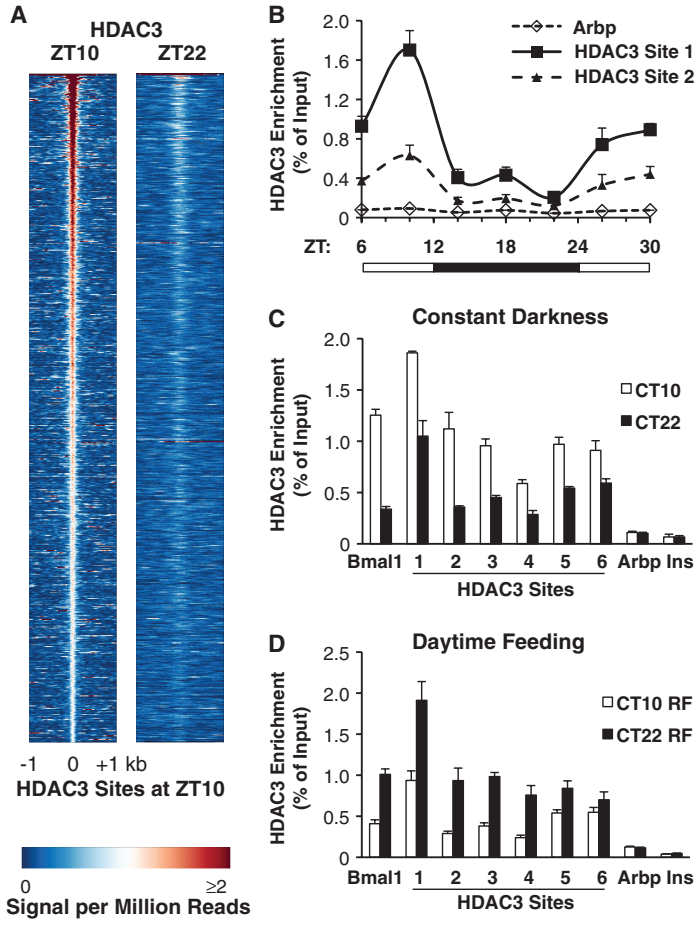

Fig. 1. Circadian rhythm of genomic HDAC3 recruitment in mouse liver. (**A**) Heat map of HDAC3 binding signal at ZT10 (left) and ZT22 (right) from −1 kb to +1 kb surrounding the center of all the HDAC3 ZT10 binding sites, ordered by strength of HDAC3 binding at ZT10. ChIP-seq with antibody against HDAC3 (anti-HDAC3) was performed, and data were analyzed as described in (*31*). Each line represents a single HDAC3 binding site, and the color scale indicates the HDAC3 signal (reads encompassing each locus per million total reads). A read is a unique sequence obtained in ChIP-seq and then aligned to the mouse genome. ZT, Zeitgeber time (light on at ZT0, off at ZT12). (**B**) HDAC3 recruitment at two selected genomic sites over a 24-hour cycle by ChIP–polymerase chain reaction (PCR). Immunoprecipitated DNA was normalized to input. Values are mean ± SEM (n = 4 or 5). (**C**) HDAC3 diurnal genomic recruitment is maintained in constant darkness. Six HDAC3 binding sites were assessed by ChIP-PCR (n = 4 or 5), and the *Bmal1* promoter served as a positive control (*23*); regions close to the TSS of the *Arbp* and *Ins* genes served as negative controls. CT, circadian time. (**D**) The rhythm of HDAC3 recruitment is reversed by daytime feeding (n = 4 or 5). RF, food was provided only from ZT3 to ZT11 every day for 2 weeks.

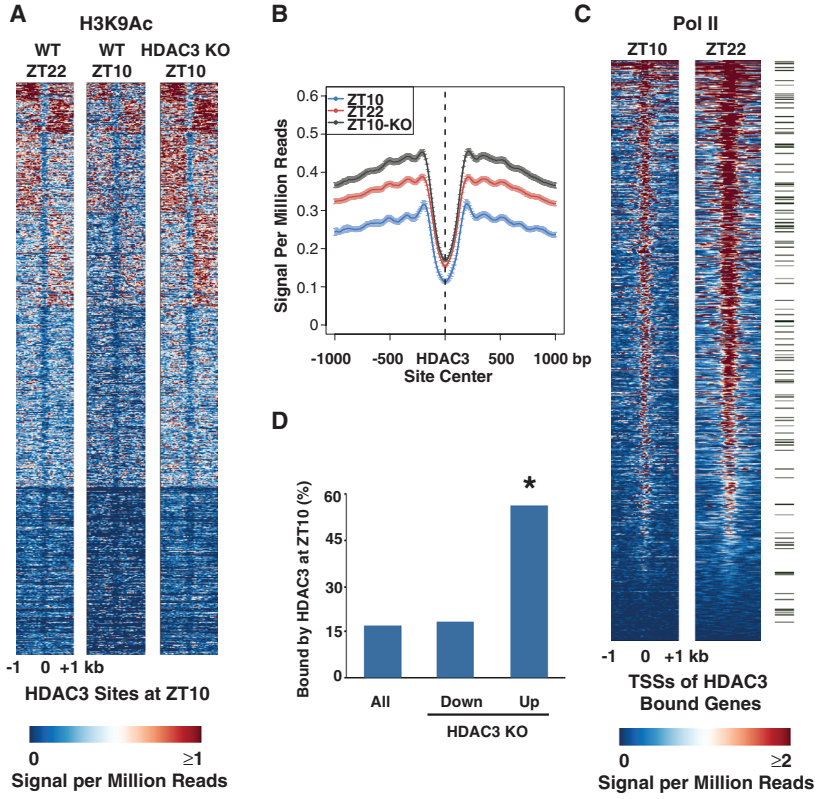

Fig. 2. Orchestration of genome-wide rhythms of histone acetylation, Pol II recruitment, and gene expression by HDAC3. (**A**) Heat map of the H3K9 acetylation (H3K9Ac) signal in WT liver at ZT22 (left), ZT10 (middle), and ZT10 in liver depleted of HDAC3 (KO) (right) from −1 kb to +1 kb surrounding the center of all the HDAC3 ZT10 binding sites, ordered by k means clustering of H3K9Ac signal. Each line represents a single HDAC3 binding site, and the color scale indicates the H3K9Ac signal per million total reads. HDAC3-depleted liver was removed from HDAC3$^{fl/fl}$ mice 1 week after injection of AAV-Cre as in (*31*). (**B**) Average H3K9Ac signal from −1 kb to +1 kb surrounding the center of all the HDAC3 ZT10 binding sites. The y axis represents the H3K9Ac signal per million total reads. bp, base pairs. (**C**) Heat map of Pol II signal at ZT10 (left) and ZT22 (right) from −1 kb to +1 kb surrounding the TSS of genes with HDAC3 recruitment within 10 kb of the TSS, ordered by strength of Pol II binding at ZT22. Each line represents a single HDAC3-bound gene, and the color scale indicates the Pol II signal per million total reads. Green marks denote 130 genes under the Gene Ontology term "Lipid Biosynthetic Process" listed in table S1. (**D**) Genes up-regulated in liver depleted of HDAC3 are significantly enriched for HDAC3 binding at ZT10. Expression arrays of WT and HDAC3 KO liver were performed and analyzed as described in (*31*), and the percentage of HDAC3-bound genes in each category was calculated. *P ~ 10^{-156} based on hypergeometic distribution as in (*31*).

recruitment has been reported to be associated with high histone acetylation, RNA polymerase II (Pol II) recruitment, and gene expression in human primary T cells (*17*). In mouse liver, HDAC3 recruitment at ZT10 was also enriched around active genes (fig. S4A), and many of these display circadian expression patterns (*18*) (fig. S4B). Thus, HDAC3 may have an important role in transient regulation of these active genes by the circadian clock. Consistent with this hypothesis, we observed decreases in acetylation of histone H3 lysine 9 (H3K9) at ZT10 compared with that at ZT22, the inverse of HDAC3 recruitment to these sites (Fig. 2, A and B). Deletion of hepatic HDAC3 by tail vein injection of adeno-associated virus expressing cre-recombinase (AAV-Cre) into adult C57Bl/6 mice homozygous for a floxed HDAC3 allele (HDAC3$^{fl/fl}$) (fig. S1A) led to H3K9 acetylation at ZT10 comparable to that of wild-type mice at ZT22 (Fig. 2, A and B). Accompanying the decreased H3K9 acetylation at ZT10 was a decrease in binding of RNA polymerase II (Pol II) at the TSS of genes with HDAC3 binding within 10 kb, indicating that they were actively repressed (Fig. 2C). Indeed, the majority of genes whose transcripts were increased 1 week after HDAC3 deletion in liver displayed HDAC3 binding within 10 kb of their TSS in WT mice at ZT10 (Fig. 2D). Thus, genome-wide diurnal recruitment of HDAC3 directs a rhythm of epigenomic modification, Pol II recruitment, and gene expression.

Although HDAC3 recruitment to the genome is diurnal, the abundance of HDAC3 was constant throughout the light/dark cycle (Fig. 3A). HDAC3 enzyme activity requires interaction with nuclear receptor (NR) corepressors (*19*), and de novo motif analysis of the HDAC3 binding sites revealed the classical motif recognized by a number of NRs (fig. S5). The NR Rev-erbα is a transcriptional repressor that is expressed in a circadian manner (*20*), and the abundance of Rev-erbα protein oscillated in phase with HDAC3 recruitment (Fig. 3A). We used a Rev-erbα–specific antibody (fig. S6A) to determine the Rev-erbα binding sites (fig. S6, B and C). At ZT10, the Rev-erbα binding sites overlapped with the majority of HDAC3 binding sites (Fig. 3B). Furthermore, Rev-erbα bound to the majority of HDAC3 ZT10 sites at ZT10 but not ZT22 (Fig. 3C). The extent of overlap of HDAC3 with Rev-erbα was surprising given that other NRs can interact with corepressors and HDAC3 (*21*). However, HDAC3 recruitment was diminished at many sites in Rev-erbα knockout (KO) mice (Fig. 3D), consistent with a critical role for Rev-erbα, although residual HDAC3 binding suggests that other factors also contribute to its recruitment. Rev-erbα recruits HDAC3 via the nuclear receptor corepressor (NCoR) (*22*, *23*). NCoR was recruited to HDAC3 sites with a diurnal rhythm (Fig. 3C), which was attenuated in the Rev-erbα KO mice (Fig. 3E). Moreover, HDAC3 bound together with NCoR as well as Rev-erbα at the majority of ZT10 sites (fig. S7).

We addressed the biological role of the circadian genomic recruitment of HDAC3 in mouse liver. The set of genes bound by Rev-erbα and HDAC3, and up-regulated in livers depleted of HDAC3, was enriched for genes encoding proteins that function in lipid metabolic processes (Fig. 4A). Indeed, in liver of chow-fed mice in which HDAC3 was deleted for 2 weeks, Oil Red O staining for neutral lipid was dramatically increased (Fig. 4B), and liver triglyceride content was increased nearly 10-fold (Fig. 4C), with serum transaminase activity increasing only modestly (fig. S8A). This was consistent with a fatty liver phenotype of mice depleted of hepatic HDAC3 in utero (*24*) (fig. S9).

The majority of genes up-regulated in liver depleted of Rev-erbα (*25*) were bound by HDAC3 as well as Rev-erbα at ZT10 (fig. S10). Indeed, chow-fed C57Bl/6 mice genetically lacking Rev-erbα (*26*) had normal serum transaminase activity (fig. S8B), but Oil Red O staining of liver was increased (Fig. 4D) and hepatic triglyceride content was nearly double that of wild-type mice (Fig. 4E). The relatively modest hepatic steatosis in the Rev-erbα–deleted mice likely reflects a role for HDAC3 in mediating effects of

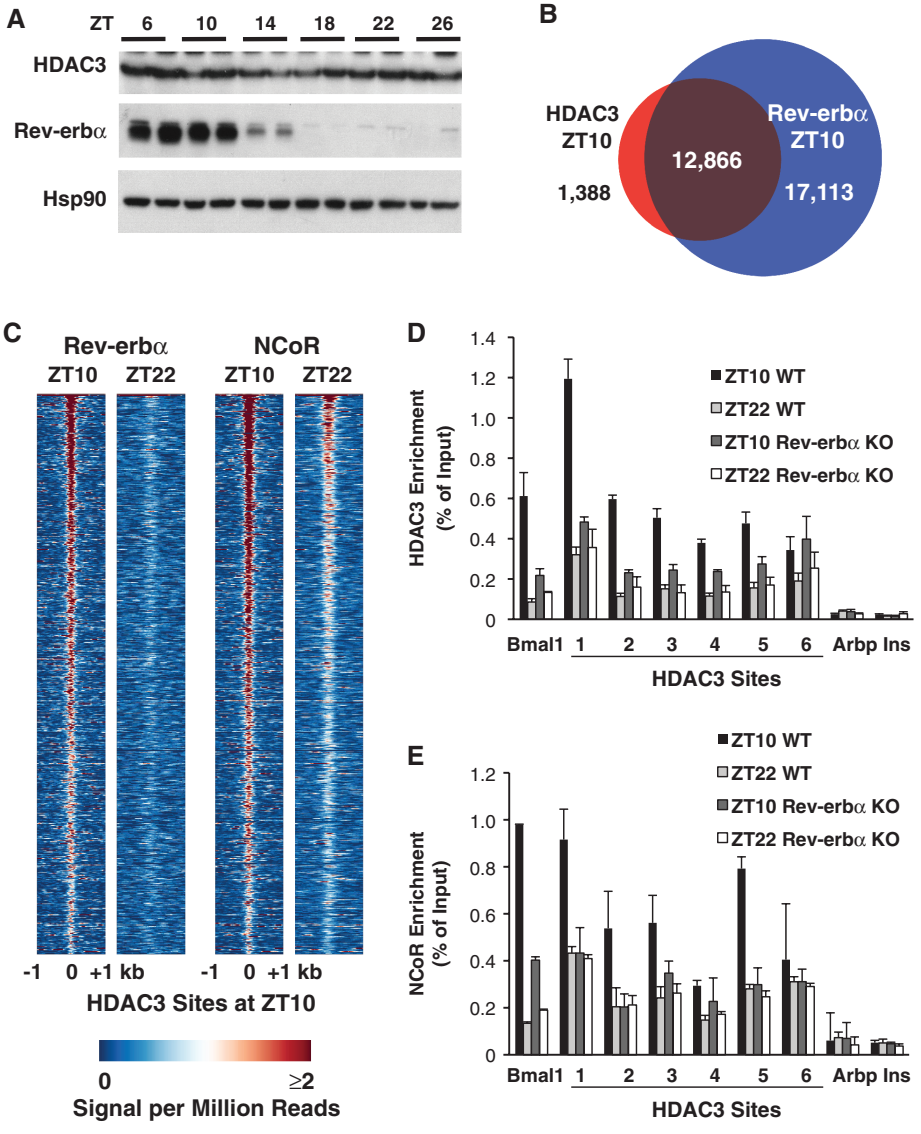

Fig. 3. Recruitment of HDAC3 to the genome by Rev-erbα. (**A**) Immunoblot of HDAC3 and Rev-erbα over a 24-hour cycle in mouse liver. Heat shock protein 90 (Hsp90) levels are shown as loading control. (**B**) The HDAC3 cistrome at ZT10 largely overlaps with the Rev-erbα cistrome at ZT10. ChIP-seq with anti-Rev-erbα was performed and analyzed as described in (*31*). (**C**) Heat map of Rev-erbα at ZT10 and ZT22 (left) and of NCoR at ZT10 and ZT22 (right), both at HDAC3 ZT10 sites ordered as in Fig. 1A. Each line represents a single HDAC3 binding site, and the color scale indicates the signal per million total reads. (**D** and **E**) HDAC3 (D) and NCoR (E) recruitment to six binding sites (as in Fig. 1C) were interrogated by ChIP-PCR in liver from mice lacking Rev-erbα. The *Bmal1* promoter was used as a positive control (*23*); regions close to the TSS of the *Arbp* and *Ins* genes served as negative controls. Values are mean ± SEM (n = 3).

other NRs—including Rev-erbβ, whose circadian expression pattern is similar to that of Rev-erbα (*27*)—but could also reflect a compensatory effect of Rev-erbα KO in other tissues. Nevertheless the finding that depletion of either Rev-erbα or HDAC3 led to a fatty liver phenotype supports the conclusion that circadian Rev-erbα recruitment of HDAC3 to lipid metabolic genes plays a critical physiological role.

Rev-erbα and HDAC3 colocalized at >100 lipid biosynthetic genes at ZT10, including *Fasn* and *Acaca* (table S1), and Pol II recruitment increased from ZT10 to ZT22 at the TSS of many of these genes (Fig. 2C), suggesting that they were directly repressed. Assessment of palmitate synthesis after injection of deuterated water revealed increased de novo lipogenesis in mice lacking hepatic HDAC3 (Fig. 4F) and in Rev-erbα KO mice (fig. S11), thus revealing a molecular mechanism underlying the observation that hepatic lipogenesis in mice follows a diurnal rhythm (*28*) that is antiphase to Rev-erbα and HDAC3 recruitment to the mouse genome.

These findings demonstrate the existence of circadian changes in histone acetylation whose dysregulation has the potential to cause major perturbations in normal metabolic function. Each day, low concentrations of Rev-erbα lead to reduced HDAC3 association with the liver genome while the organism is active and feeding, altering the epigenome to permit lipid synthesis and accumulation until abundance of Rev-erbα increases HDAC3 recruitment to liver metabolic genes and halts the lipid build-up (Fig. 4G). When either Rev-erbα or HDAC3 is depleted, this cycle does not occur, and fatty liver ensues. Misalignment of fasting/feeding and sleep/wake cycles with endogenous circadian cycles could disrupt the rhythm of HDAC3 association with target genes and contribute to the fatty liver observed in rotating shift workers as well as people with genetic variants of molecular clock genes (*29*, *30*).

A

Genes bound by HDAC3 and Rev-erbα and up-regulated in HDAC3 KO

Biological Processes	p-value
Lipid metabolic process	1.72E-24
Metabolic process	8.22E-21
Cellular amino acid and derivative metabolic process	8.33E-19
Primary metabolic process	8.30E-17
Coenzyme metabolic process	1.84E-14
Carbohydrate metabolic process	1.78E-11

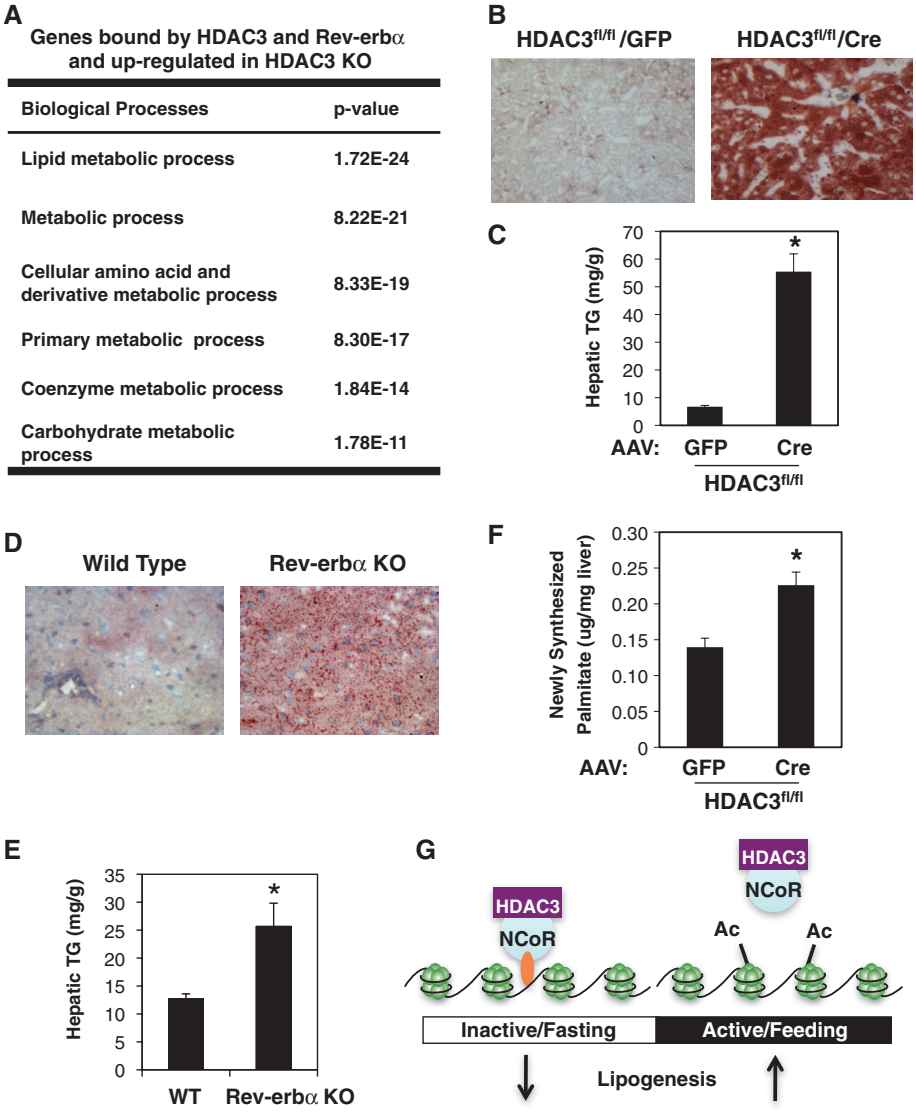

Fig. 4. Regulation of hepatic lipid homeostasis by HDAC3. (**A**) Gene Ontology analysis of the HDAC3- and Rev-erbα–bound genes that were up-regulated in liver depleted of HDAC3 was performed as described in (*31*). (**B**) Oil Red O staining of liver from 12-week-old HDAC3$^{fl/fl}$ mice 2 weeks after tail vein injection of AAV–green fluorescent protein (GFP) or AAV-Cre. (**C**) Hepatic triglyceride (TG) levels in mice treated as in (B). (**D**) Oil Red O staining of livers from 9-week-old WT and mice lacking Rev-erbα (Rev-erbα KO). (**E**) Hepatic TG levels in livers from 9-week-old WT and Rev-erbα KO. Values are mean ± SEM (n = 4). *P < 0.05 by Student's t test. (**F**) Hepatic de novo lipogenesis (DNL) in 12-week-old HDAC3$^{fl/fl}$ mice 1 week after infection with AAV-Cre or with AAV-GFP. Hepatic DNL is measured as newly synthesized ^{2}H-labeled palmitate. Values are mean ± SEM (n = 7 or 8). *P < 0.05 by Student's t test. (**G**) Model depicting the mechanistic links between the daily cycles of Rev-erbα expression (orange oval), HDAC3 genomic recruitment, epigenomic status, and hepatic lipogenesis.

References and Notes

1. C. B. Green, J. S. Takahashi, J. Bass, *Cell* **134**, 728 (2008).
2. E. Maury, K. M. Ramsey, J. Bass, *Circ. Res.* **106**, 447 (2010).
3. F. A. Scheer, M. F. Hilton, C. S. Mantzoros, S. A. Shea, *Proc. Natl. Acad. Sci. U.S.A.* **106**, 4453 (2009).
4. A. Pietroiusti *et al.*, *Occup. Environ. Med.* **67**, 54 (2010).
5. D. De Bacquer *et al.*, *Int. J. Epidemiol.* **38**, 848 (2009).
6. B. Marcheva *et al.*, *Nature* **466**, 627 (2010).
7. F. W. Turek *et al.*, *Science* **308**, 1043 (2005); 10.1126/science.1108750.
8. K. A. Lamia, K. F. Storch, C. J. Weitz, *Proc. Natl. Acad. Sci. U.S.A.* **105**, 15172 (2008).
9. K. Eckel-Mahan, P. Sassone-Corsi, *Nat. Struct. Mol. Biol.* **16**, 462 (2009).
10. R. D. Rudic *et al.*, *PLoS Biol.* **2**, e377 (2004).
11. S. Panda *et al.*, *Cell* **109**, 307 (2002).
12. J. P. Etchegaray, C. Lee, P. A. Wade, S. M. Reppert, *Nature* **421**, 177 (2003).
13. M. Doi, J. Hirayama, P. Sassone-Corsi, *Cell* **125**, 497 (2006).
14. B. D. Strahl, C. D. Allis, *Nature* **403**, 41 (2000).
15. T. Alenghat *et al.*, *Nature* **456**, 997 (2008).
16. F. Damiola *et al.*, *Genes Dev.* **14**, 2950 (2000).
17. Z. Wang *et al.*, *Cell* **138**, 1019 (2009).
18. M. E. Hughes *et al.*, *PLoS Genet.* **5**, e1000442 (2009).
19. M. G. Guenther, O. Barak, M. A. Lazar, *Mol. Cell. Biol.* **21**, 6091 (2001).
20. N. Preitner *et al.*, *Cell* **110**, 251 (2002).
21. M. Goodson, B. A. Jonas, M. A. Privalsky, *Nucl. Recept. Signal.* **3**, e003 (2005).
22. I. Zamir *et al.*, *Mol. Cell. Biol.* **16**, 5458 (1996).
23. L. Yin, M. A. Lazar, *Mol. Endocrinol.* **19**, 1452 (2005).
24. S. K. Knutson *et al.*, *EMBO J.* **27**, 1017 (2008).
25. B. Kornmann, O. Schaad, H. Bujard, J. S. Takahashi, U. Schibler, *PLoS Biol.* **5**, e34 (2007).
26. P. Chomez *et al.*, *Development* **127**, 1489 (2000).
27. A. C. Liu *et al.*, *PLoS Genet.* **4**, e1000023 (2008).
28. D. A. Hems, E. A. Rath, T. R. Verrinder, *Biochem. J.* **150**, 167 (1975).
29. E. M. Brunt, *Nat. Rev. Gastroenterol. Hepatol.* **7**, 195 (2010).
30. S. Sookoian, G. Castaño, C. Gemma, T. F. Gianotti, C. J. Pirola, *World J. Gastroenterol.* **13**, 4242 (2007).
31. Materials and methods are available as supporting material on *Science* Online.

32. ChIP-seq and microarray data have been deposited in the Gene Expression Omnibus (GSE25937 and GSE26345) database. We thank B. Vennström for providing Rev-erbα KO mice; M. Brown, D. Steger, and members of the Lazar lab for helpful discussions; D. Zhuo for technical assistance; the Penn IDOM Metabolism Resource (J. Millar) for help with de novo lipogenesis experiments; the Functional Genomics Core (J. Schug and K. Kaestner) and the Viral Vector Core (J. Johnston) of the Penn Diabetes Endocrinology Research Center (NIH DK19525) for deep sequencing and virus preparation; the Morphology Core (J. Katz and G. Swain) (NIH DK49210) for tissue preparation and staining; and the Penn Bioinformatics Core (J. Tobias) and Microarray Core (D. Baldwin) for gene expression analysis. Supported by the Cox Institute, NIH DK45586, DK43806, and RC1DK08623 (to M.A.L.) and NIH HG4069 (to X.S.L.).

Supporting Online Material
www.sciencemag.org/cgi/content/full/331/6022/1315/DC1
Materials and Methods
Figs. S1 to S11
Tables S1 to S3
References

22 September 2010; accepted 6 January 2011
10.1126/science.1198125

A Bacterial Protein Targets the BAHD1 Chromatin Complex to Stimulate Type III Interferon Response

Alice Lebreton,[1,2,3] Goran Lakisic,[4] Viviana Job,[5] Lauriane Fritsch,[6] To Nam Tham,[1,2,3] Ana Camejo,[7] Pierre-Jean Matteï,[5] Béatrice Regnault,[8] Marie-Anne Nahori,[1,2,3] Didier Cabanes,[7] Alexis Gautreau,[4] Slimane Ait-Si-Ali,[6] Andréa Dessen,[5] Pascale Cossart,[1,2,3]* Hélène Bierne[1,2,3]*

Intracellular pathogens such as *Listeria monocytogenes* subvert cellular functions through the interaction of bacterial effectors with host components. Here we found that a secreted listerial virulence factor, LntA, could target the chromatin repressor BAHD1 in the host cell nucleus to activate interferon (IFN)–stimulated genes (ISGs). IFN-λ expression was induced in response to infection of epithelial cells with bacteria lacking LntA; however, the BAHD1-chromatin associated complex repressed downstream ISGs. In contrast, in cells infected with *lntA*-expressing bacteria, LntA prevented BAHD1 recruitment to ISGs and stimulated their expression. Murine listeriosis decreased in *BAHD1*$^{+/-}$ mice or when *lntA* was constitutively expressed. Thus, the LntA-BAHD1 interplay may modulate IFN-λ–mediated immune response to control bacterial colonization of the host.

Listeria monocytogenes is a food-borne pathogen that can cause serious illness in pregnant women and immunocompromised individuals (*1*). This intracellular bacterium uses an arsenal of effectors to exploit cellular functions in various ways (*2*). Host cells respond to this invasion by turning on appropriate defense transcriptional programs (*3*). *Listeria* and other pathogens can manipulate chromatin to reprogram host transcription (*4*, *5*). However, very few bacterial molecules have been shown to enter eukaryotic cell nuclei, and knowledge about microbial factors that may act directly on the chromatin-regulatory machinery is limited (*6*).

To identify factors involved in bacterial pathogenicity, we screened the *L. monocytogenes* strain EGDe genome for genes encoding secreted proteins absent in nonpathogenic *Listeria* species. *lmo0438*/*lntA* (listeria nuclear targeted protein A) was one such gene (fig. S1A). *lntA* was expressed at very low levels by the EGDe strain grown in brain-heart infusion (BHI) medium (fig. S1B) (*7*). Two major regulators of virulence genes, PrfA and σ^B, were required for basal *lntA* transcription (Fig. 1A). *lntA* expression was significantly higher in bacteria harvested from spleens of infected mice, 48 hours after intravenous inoculation, compared with that of bacteria grown in BHI (Fig. 1B). In addition, deletion of *lntA* led to a decrease in bacterial colonization of spleens and livers, as well as blood bacteraemia (Fig. 1B). *lntA* thus contributes to *L. monocytogenes* virulence. It encodes a 205–amino acid basic protein with a N-terminal signal peptide but no sequence similarity with any known polypeptide. The 2.3 Å resolution structure of LntA reveals a compact α-helical fold (fig. S2) [Protein Data Bank (PDB) ID no. 2xl4]. Consistent with low *lntA* transcription levels in vitro, LntA was undetectable in either total extracts or supernatants of wild-type (WT) bacteria grown in BHI (Fig. 1C).

To address the role of LntA during *L. monocytogenes* cellular infection, we generated strains that constitutively expressed *lntA* under the control of a heterologous promoter, either on the chromosome (*lntA*$^{c+}$) or on a plasmid in fusion with the V5 tag (*lntA*$^{V5+}$) (tables S1 and S2). Both strains produced and secreted LntA (Fig. 1C and fig. S1C) and showed no noticeable difference in entry or multiplication in cultured cells compared with the WT or *lntA*-deficient strains (Δ*lntA*, *lntA*$^-$, or *lntA*$^{c-}$) (table S3A and fig. S3). Secreted LntA accumulated in the nucleus of fibroblasts after 22 hours of infection with *lntA*$^{V5+}$ bacteria (Fig. 1D and fig. S4A). We thus assessed whether LntA interacted with nuclear proteins in a large-scale yeast two-hybrid screen of a human cDNA library. One of the strongest LntA interactors was BAHD1, a silencing factor that orchestrates heterochromatin assembly at specific genes such as that for insulin-like growth factor 2 *IGF2* (*8*). A fusion of LntA with glutathione *S*-transferase (GST) pulled down V5-tagged BAHD1 from nuclear extracts, which confirmed the capacity of LntA to specifically interact with BAHD1 (Fig. 1E). When produced ectopically in human fibroblasts, LntA colocalized with heterochromatin nuclear foci that were induced by overexpression of BAHD1 tagged with yellow fluorescent protein (BAHD1-YFP) (*8*), both in fixed (LntA-V5) (Fig. 1F) and in living cells (LntA tagged with cyan fluorescent protein, LntA-CFP) (fig. S4B).

Because BAHD1 is involved in gene silencing, LntA might control host gene expression. To assess this hypothesis, we performed a transcriptome analysis of colon carcinoma epithelial LoVo cells infected for 24 hours with either *lntA*$^{V5+}$ or *lntA*$^-$ bacteria (GEO database, GSE26414). The *lntA*$^{V5+}$ bacteria specifically up-regulated the expression of a subset of genes, out of which 39 displayed a more than twofold induction (table S4). Of these genes, 83% belonged to the interferon-inducible genes regulon: 28 are known interferon-stimulated genes (ISGs), including three genes (*IL29*, *IL28A*, and *IL28B*) that encode type III interferons (IFN-λ1, -λ2, and -λ3), and four are predicted ISGs. LntA may thus play a role in the IFN-III–mediated immune response. This pathway controls various viral infections, especially in epithelial tissues (*9*–*13*).

We confirmed that WT *L. monocytogenes* triggered the expression of *IFN-λ2* in intestinal LoVo and placental JEG-3 epithelial cells (Fig. 2A and fig. S5A), while type I *IFN-β1* was induced a little and type II *IFN-γ* was undetectable. However, the induction of downstream ISGs was modest (Fig. 2A), except for *CCL5*, which, like *IFN-λ* genes, is controlled both by nuclear factor κB (NF-κB) and interferon regulatory factors (IRFs) (*14*). These data suggested that interferon signaling was down-regulated in infected cells. We wondered whether the host factor BAHD1 could act as a repressor of ISGs, as it does for *IGF2* (fig. S5B) (*8*). Knockdown (depletion) of *BAHD1* had no or minor effect on ISG expression

[1]Institut Pasteur, Unité des Interactions Bactéries Cellules, Paris F-75015, France. [2]Inserm, U604, Paris F-75015, France. [3]INRA, USC2020, Paris F-75015, France. [4]CNRS UPR3082, Laboratoire d'Enzymologie et de Biochimie Structurales, Gif-sur-Yvette F-91198, France. [5]Institut de Biologie Structurale, Bacterial Pathogenesis Group, UMR 5075 (CNRS/CEA/UJF), Grenoble F-38027, France. [6]CNRS UMR7216, Université Paris Diderot-Paris 7, Paris F-75013, France. [7]Institute for Molecular and Cellular Biology, Porto 4150, Portugal. [8]Institut Pasteur, Génopole, Paris F-75015, France.

*To whom correspondence should be addressed. E-mail: hbierne@pasteur.fr (H.B.); pcossart@pasteur.fr (P.C.)